NMR-like Control of a Quantum Bit Superconducting Circuit

E. Collin, G. Ithier, A. Aassime, P. Joyez, D. Vion, and D. Esteve

Quantronics group, Service de Physique de l'Etat Condensé, DSM/DRECAM, CEA Saclay, 91191 Gif-sur-Yvette, France

(Received 17 March 2004; published 6 October 2004)

Coherent superpositions of quantum states have already been demonstrated in different superconducting circuits based on Josephson junctions. These circuits are now considered for implementing quantum bits. We report on experiments in which the state of a qubit circuit, the quantronium, is efficiently manipulated using methods inspired from nuclear magnetic resonance (NMR): multipulse sequences are used to perform arbitrary operations, to improve their accuracy, and to fight decoherence.

DOI: 10.1103/PhysRevLett.93.157005 PACS numbers: 85.25.Cp, 03.67.Lx, 74.50.+r, 74.78.Na

Despite progress in the development of quantum bit (qubit) electronic circuits, the complexity and robustness of the operations that have been performed on them are presently still too primitive for demonstrating quantum computing (QC) [1]. Presently, the most advanced qubit circuits are superconducting ones based on Josephson junctions. The preparation of coherent superpositions of the two states of a qubit has already been demonstrated for several circuits [2–9], and a two qubit gate was operated [10]. However, qubit operations are far less developed for qubit circuits than for atoms or spins. In this Letter, we report on experiments that successfully manipulate a Josephson qubit based on the quantronium circuit [11], using NMR methods. We demonstrate that any transformation of the qubit can be implemented, that they can be made robust, and that decoherence can be fought. Note that using NMR methods for qubit manipulation does not bring in the intrinsic limitations of QC with nuclear spins, such as the lack of scalability, because in this approach the NMR sequence is applied to a single distinguishable qubit, not to an ensemble.

The quantronium circuit, described in Fig. 1, is derived from the Cooper pair box [12,13]. It consists of a superconducting loop interrupted by two adjacent small Josephson tunnel junctions with Josephson energy $E_J/2$ each, and by a larger Josephson junction ($E_{J0} \approx 15E_J$) for readout. The island between the small junctions, with total capacitance C_Σ and charging energy $E_C = (2e)^2/2C_\Sigma$, is biased by a voltage source U through a gate capacitance C_g. The characteristic energies measured in the present sample are $E_J = 0.87k_B$ K and $E_C = 0.66k_B$ K. Experiments are performed at 20 mK using filtered lines. The eigenstates of this system are determined by the dimensionless gate charge $N_g = C_g U/2e$, and by the superconducting phase $\delta = \gamma + \phi$ across the two small junctions, where γ is the phase across the large junction and $\phi = \Phi/\varphi_0$, with Φ the external flux through the loop and $\varphi_0 = \hbar/2e$. The two lowest energy states $|0\rangle$ and $|1\rangle$ form a two-level system suitable for a qubit. At the optimal working point ($\delta = 0, N_g = 1/2$), the transition frequency ν_{01} is stationary with respect to changes in the control parameters, which makes the quantronium insensitive to noise at first order [3,11]. For the sample investigated, $\nu_{01} \simeq 16.40$ GHz at the optimal working point. For readout, $|0\rangle$ and $|1\rangle$ are discriminated through the difference in their supercurrents in the loop [3]. A trapezoidal readout pulse $I_b(t)$ with a peak value slightly below

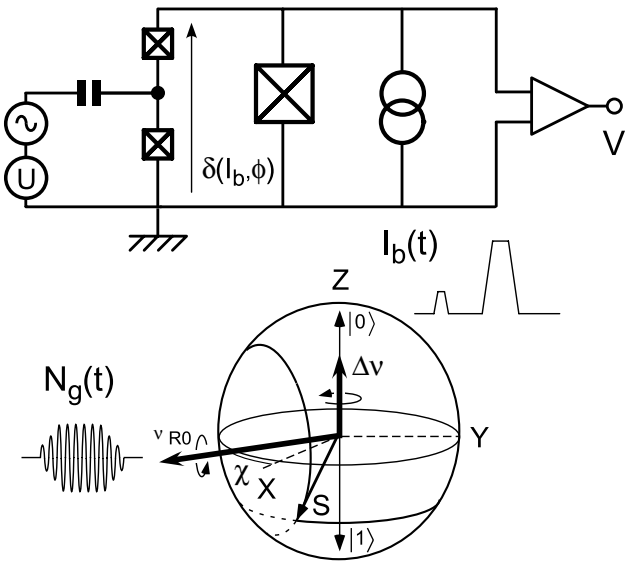

FIG. 1. Top: quantronium circuit. The Hamiltonian is controlled by the gate charge N_g applied to the island between the two small junctions, and by the phase δ across their series combination. This phase is determined by the flux ϕ through the loop, and by the bias current I_b. The two lowest energy states form a two-level system suitable for a qubit. The readout is performed by inducing the switching of the larger readout junction to a finite voltage V with a bias-current pulse $I_b(t)$ approaching the critical current of this junction. Bottom: The quantum state is manipulated by applying resonant microwave pulses (phase χ) on the gate, or adiabatic pulses on the bias current. These pulses induce a rotation of the effective spin $\vec{S}$ representing the qubit state on the Bloch sphere in the rotating frame. The Rabi precession of $\vec{S}$ during a microwave pulse results in oscillations of the switching probability p with the pulse length τ.

the critical current $I_0 = E_{J0}/\varphi_0 \simeq 450$ nA is applied so that the switching of the large junction to a finite voltage state is induced with a large probability p_1 for state $|1\rangle$ and with a small probability p_0 for state $|0\rangle$. The switching is detected by measuring the voltage across the readout junction, and p is determined by repeating the experiment a few 10^4 times. The fidelity η of the measurement is the largest achieved value of $p_1 - p_0$.

The manipulation of the qubit state is achieved by applying time dependent control parameters $N_g(t)$ and $I_b(t)$. When a nearly resonant microwave modulation $\Delta N_g \cos(2\pi\nu_{\mu w}t + \chi)$ is applied to the gate, the Hamiltonian described in a frame rotating at the microwave frequency $h = -\vec{H}\cdot\vec{\sigma}/2$ is that of a spin 1/2 in an effective magnetic field $\vec{H} = h\Delta\nu\vec{z} + h\nu_{R0}[\vec{x}\cos\chi + \vec{y}\sin\chi]$, where $\Delta\nu = \nu_{\mu w} - \nu_{01}$ is the detuning, and $\nu_{R0} = 2E_C\Delta N_g\langle 1|\hat{N}|0\rangle/h$ the Rabi frequency. At $\Delta\nu = 0$, Rabi precession takes place around an axis lying in the equatorial plane, at an angle χ with respect to the X axis. Rabi precession induces oscillations of the switching probability p with the pulse duration [3]. The range of Rabi frequencies ν_{R0} that could be explored extends above 250 MHz, and the shortest π pulse duration for preparing $|1\rangle$ starting from $|0\rangle$ was less than 2 ns. The fidelity was $\eta \simeq 0.3$–0.4 for readout pulses with 100 ns duration at the optimal value of δ at readout. This fidelity might be improved using rf methods that avoid switching to the voltage state [14].

In order to perform arbitrary operations on the qubit, one has to combine rotations around different axes [1], i.e., pulses with different phases. For that purpose, a continuous microwave signal is divided on two lines, one being phase shifted as desired. Both lines are fed to mixers controlled by dc pulses, and then recombined and applied to the gate. In Fig. 2, measurements of the switching probability p following two-pulse sequences combining $\pi/2$ rotations around the axes $X, Y, -X$, or $-Y$, are shown. Theory predicts that p oscillates at frequency $\Delta\nu$ with the delay Δt between pulses. This experiment is analogous to the Ramsey experiment in atomic physics, and to the free induction decay in NMR. When the two pulses have different phases χ_1 and χ_2, the Ramsey pattern is phase- shifted by $\chi_2 - \chi_1$. Despite the presence of spurious frequency jumps due to individual charge fluctuators near the island, the overall agreement for the phase shift of the Ramsey pattern demonstrates that rotations around axes X and Y combine as predicted. Arbitrary unitary transformations can thus be performed. Rotations around the Z axis can, however, be more readily performed by changing the qubit frequency for a short time. A triangular bias-current pulse with maximum amplitude ΔI is applied in a Ramsey experiment. During this detuning pulse, a phase difference $\zeta = 2\pi\int\delta\nu_{01}(t)dt$ builds up between the qubit states, which is equivalent to a rotation around the Z axis with an angle ζ. The Ramsey pattern is phase shifted

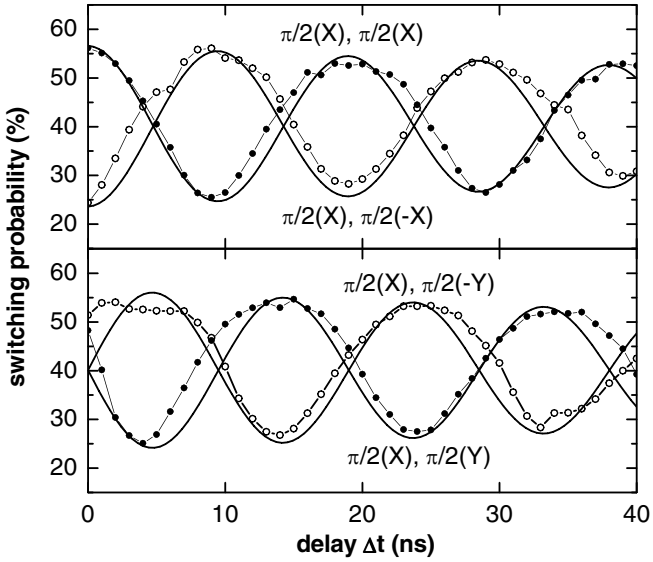

FIG. 2. Switching probability after two $\pi/2$ pulses with detuning $\Delta\nu = +52$ MHz, and with different phases corresponding to rotation axes X, Y, $-X$, or $-Y$, as a function of the delay between the pulses. The solid lines are fits including a finite decay time of 250 ns. The Ramsey patterns are phase shifted as predicted for the different combinations of rotation axes.

by ζ as shown by the oscillations of p with ΔI (right panel of Fig. 3).

The accuracy and robustness of these qubit operations are also important issues. In NMR, composite pulse methods have been developed to make such manipulations less sensitive to rf pulse imperfections [15,16]. In the case of the CORPSE sequence (compensation for off-resonance with a pulse sequence), the sensitivity to de-

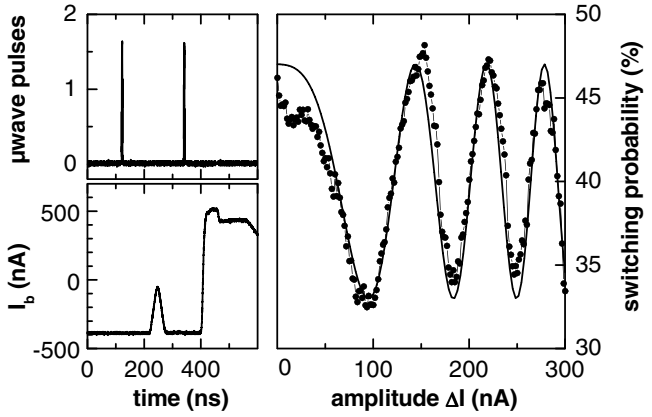

FIG. 3. Demonstration of rotations around the Z axis. Left: a triangular bias-current pulse applied between the two pulses of a Ramsey sequence induces a frequency change, and thus a phase shift between the two qubit states. Right: this phase shift, equivalent to a rotation around the Z axis, results in oscillations of the switching probability p (symbols) with the pulse amplitude ΔI. The fit (thick line) uses the measured dependence of the transition frequency with the phase δ.

tuning is strongly reduced, the error starting at fourth order. We have tested this sequence in the case of a π rotation around the X axis, which performs a NOT operation on the qubit. The corresponding CORPSE $\pi(X)$ pulse sequence is $\{7\pi/3(X), 5\pi/3(-X), \pi/3(X)\}$ [15]. As shown in Fig. 4, it is significantly more robust against detuning than a single pulse $\pi(X)$ since the switching probability stays close to its maximum value over a larger frequency range, comparable to the Rabi frequency. By performing the CORPSE sequence after an arbitrary rotation $\theta(-X)$, we have also checked that the sequence works for a general initial state.

Another major concern of qubit circuits is to improve quantum coherence, which is limited by relaxation and dephasing. The relaxation time T_1 was 500 ± 50 ns at the optimal working point. The lifetime of coherent superpositions is given by the decay of the Ramsey oscillations. This decay was close to exponential with $T_2 = 300 \pm 50$ ns for the present sample at the optimal working point (see top panel of Fig. 5), showing that dephasing dominates decoherence. T_2 becomes progressively shorter when the working point is moved away [3]. NMR concepts are again useful for fighting decoherence. First, the well known spin-echo technique [17] suppresses the effect of slow variations of the qubit frequency [5]. By inserting a π pulse in the middle of a Ramsey sequence, the random phases accumulated during the two free evolution periods before and after the π pulse cancel provided that the perturbation is almost static on the time scale of the sequence. The echo method thus provides a simplified form of error correction between an initial time and a final one. As shown in Fig. 5 (middle panel), we have recorded echoes, and the echo minimum at the nominal echo position as a function of the total sequence duration. The small residual oscillations on the echo mimimum result from the finite duration of the pulses and from a slight residual detuning, and simulations taking these effects into account, show that the echo decay time T_E is the decay time of the envelope of these oscillations. At the optimal point, we find $T_E = 550 \pm 50$ ns $\sim 2T_2$, which agrees with the prediction for the second order contribution of the charge noise, propor-

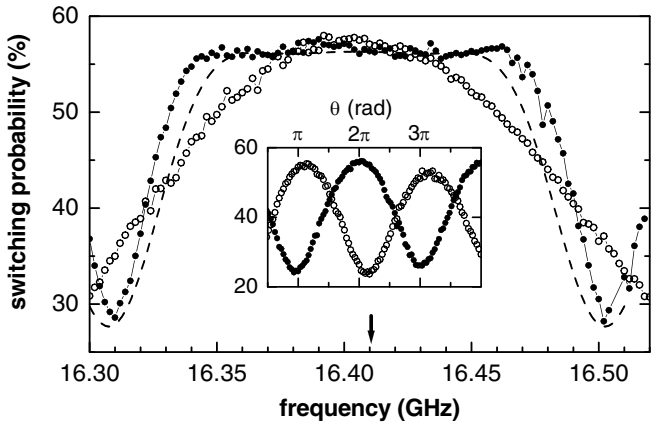

FIG. 4. Demonstration of the robustness of a composite pulse with respect to frequency detuning: switching probability after a CORPSE $\pi(X)$ sequence (disks), and after a single $\pi(X)$ pulse (circles). The dashed line is the prediction for the CORPSE, and the arrow indicates the qubit transition frequency. The CORPSE sequence works over a larger frequency range. The Rabi frequency was 92 MHz. Inset: oscillations of the switching probability after a single pulse $\theta(-X)$ followed (disks) or not (circles) by a CORPSE $\pi(X)$ pulse. The patterns are phase shifted by π as predicted.

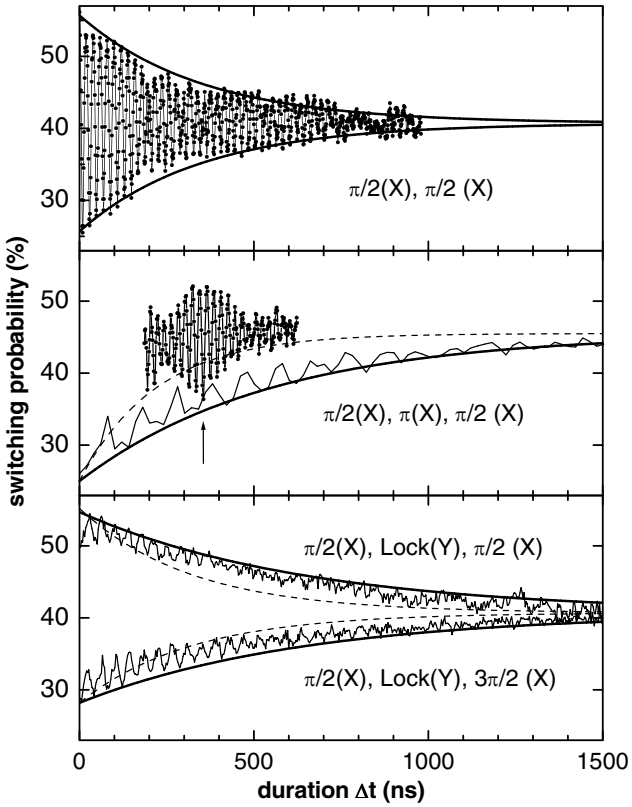

FIG. 5. Top panel: switching probability (dots) after a Ramsey $\{\pi/2(X), \pi/2(X)\}$ sequence at $\Delta\nu = +50$ MHz, as a function of the time delay between pulses. The lines are exponential fits of the envelope with a time constant $T_2 = 350$ ns. Middle panel: example of echo measured with a $\{\pi/2(X), \pi(X), \pi/2(X)\}$ sequence by increasing only the delay between the first $\pi/2$ and the π pulses (dots). The arrow indicates the nominal position of the echo minimum. Thin line: echo signal at the nominal minimum position, obtained by increasing the total sequence duration, while keeping the π pulse precisely in the middle. The bold line is an exponential fit of the envelope with a 550 ns time constant. The dashed line shows a fit of the lower envelope of the Ramsey pattern measured in the same conditions (220 ns time constant). Bottom panel: switching probability (thin lines) after two spin-locking sequences with a Rabi locking frequency of 24 MHz, at the optimal working point, versus sequence duration. Thick lines: exponential fits of the envelopes, with time constant 650 ns (see text). The dashed lines show a fit of the envelope of the Ramsey pattern measured in the same conditions (time constant: 320 ns).

tional to the second derivative $\partial^2 \nu_{01}/\partial N_g^2$. Although T_2 and T_E are 2 orders of magnitude longer than found in Ref. [2] using dc gate-charge pulses and a continuous measurement, the echo efficiencies T_E/T_2 in the two experiments are comparable. Theoretically, the effect of charge noise could be further reduced by using larger values of E_J/E_C, at the expense of reduced anharmonicity.

Another way to increase the effective coherence time is to continuously drive the qubit with a microwave signal. The dynamics of the qubit then takes place in the rotating frame, with times T_1 and T_2 being replaced by $\tilde{T}_1$ and $\tilde{T}_2$. The time $\tilde{T}_1$ is measured in a spin-locking sequence, which consists of a Ramsey sequence with a driving locking field along the direction Y or $-Y$ continuously applied between the two $\pi/2(X)$ pulses. The state $|-Y\rangle$ prepared by the first pulse is thus an eigenstate of the Hamiltonian in the rotating frame, and only its phase evolves in time. Depolarization of the states $|-Y\rangle$ and $|Y\rangle$ occur under the effect of fluctuations at the Rabi locking frequency. The bottom panel of Fig. 5 shows the decay of the signals after the two spin-locking sequences $\{\pi/2(X), \mathrm{Lock}(Y), \pm\pi/2(X)\}$. Again, small oscillations are present and due to finite pulse length and detuning. The envelope yields $\tilde{T}_1 = 650 \pm 50$ ns. Notice that $\tilde{T}_1 > T_1$ and does not depend on the orientation of the locking field along Y or $-Y$ because the energy difference between the states $|Y\rangle$ and $|-Y\rangle$ in the rotating frame is $h\nu_{R0} \ll kT$. Similarly, the decay time of the transverse part of the density matrix in the rotating frame is $\tilde{T}_2 = 480 \pm 60$ ns, deduced from the decay of Rabi oscillations for Rabi frequencies in the range (2–100 MHz) (data not shown). By encoding in the rotating frame a coherent superposition of the eigenstates, decoherence is fought, but the superposition is recovered only once per Rabi period, with an effective coherence time $\tilde{T}_2 > T_2$.

In conclusion, we have demonstrated that the state of a quantronium qubit can be efficiently manipulated using methods inspired from NMR. Rotations on the Bloch sphere around X and Y axes have been performed with microwave pulses and combined, rotations around Z have been done with adiabatic pulses, and robust rotations have been implemented using composite pulses. Finally, the spin-echo and spin-locking methods have yielded a significant reduction of decoherence. The quantitative investigation of qubit decoherence in the case of free and driven evolutions will be reported elsewhere.

We acknowledge numerous discussions in the Quantronics group, the technical help of P. F. Orfila, P. Sénat, and J. C. Tack, the support of the European project SQUBIT, of the "Action Concertée Nanosciences," and of Yale University (Grant No. DAAD 19-02-1-0044).

[1] M. A. Nielsen and I. L. Chuang, *Quantum Computation and Quantum Information* (Cambridge University Press, Cambridge, 2000).
[2] Y. Nakamura, Yu. A. Pashkin, and J. S. Tsai, Nature (London) **398**, 786 (1999); Y. Nakamura *et al.*, Phys. Rev. Lett. **88**, 047901 (2002).
[3] D. Vion *et al.*, Science **296**, 886 (2002).
[4] A. Cottet, Ph.D. thesis, Université Paris VI, 2002; www-drecam.cea.fr/drecam/spec/Pres/Quantro/.
[5] D. Vion *et al.*, Fortschr. Phys. **51**, 462 (2003).
[6] J. M. Martinis *et al.*, Phys. Rev. Lett. **89**, 117901 (2002).
[7] I. Chiorescu *et al.*, Science **299**, 1869 (2003).
[8] T. Duty *et al.*, Phys. Rev. B **69**, 140503 (2004).
[9] O. Buisson *et al.* (to be published).
[10] Yu. Pashkin *et al.*, Nature (London) **421**, 823 (2003).
[11] A. Cottet *et al.*, Physica (Amsterdam) **367C**, 197 (2002).
[12] V. Bouchiat *et al.*, Phys. Scr. **T76**, 165 (1998).
[13] Y. Nakamura, C. D. Chen, and J. S. Tsai, Phys. Rev. Lett. **79**, 2328 (1997).
[14] I. Siddiqi *et al.*, cond-mat/0312623.
[15] H. K. Cummins, G. Llewellyn, and J. A. Jones, Phys. Rev. A **67**, 042308 (2003).
[16] L. M. K. Vandersypen and I. L. Chuang, quant-ph/0404064.
[17] C. P. Slichter, *Principles of Magnetic Resonance* (Springer-Verlag, Berlin, 1990), 3rd ed.